

# In vivo cardiac <sup>1</sup>H MRS, <sup>31</sup>P MRS, and MRI in mouse models of increased fatty acid oxidation with and without myocardial lipid accumulation

Desiree Abdurrachim<sup>1</sup>, Jolita Ciapaite<sup>1</sup>, Michel van Weeghel<sup>2</sup>, Bart Wessels<sup>1</sup>, Klaas Nicolay<sup>1</sup>, Sander M. Houten<sup>2</sup>, and Jeanine J. Prompers<sup>1</sup>

<sup>1</sup>Biomedical NMR, Eindhoven University of Technology, Eindhoven, Netherlands, <sup>2</sup>Laboratory Genetic Metabolic Diseases, Academic Medical Center, Amsterdam, Netherlands

**Target Audience:** This work is relevant to the field of cardiac function and metabolism in general, and in type 2 diabetes and obesity in particular.

**Purpose:** The diabetic heart is characterized by increased fatty acid oxidation, making it less efficient in responding to changes in workload, which might result in chronic energy shortage. Despite the increase in fatty acid oxidation, the excessive availability of fatty acids in the diabetic heart exceeds the rate of oxidation, leading to myocardial lipid accumulation and lipotoxic effects. Both lipotoxicity and impaired energetics have been associated with the decreased function of the diabetic heart<sup>(1)</sup>; however, their relative contributions remain to be elucidated. The overall aim of this study was to use a combination of *in vivo* <sup>1</sup>H MRS, <sup>31</sup>P MRS, and MRI to identify the relative roles of lipotoxicity and impaired energetics in the development of cardiac dysfunction, using mouse models of increased fatty acid oxidation with and without myocardial lipid accumulation.

**Methods: Animals.** We used two different mouse models of increased fatty acid oxidation: (1) wild-type C57BL/6 mice fed with a high fat diet (45% of calories from fat) for 20 weeks (HFD; n=8), and (2) carnitine palmitoyltransferase 1b (Cpt1b) knock in mice, in which Cpt1b is rendered malonyl-CoA insensitive, fed with normal chow (Cpt1b; n=10). In contrast to HFD mice, whole-body energy balance is not affected in Cpt1b mice and it is anticipated that the hearts of Cpt1b mice will not accumulate lipids. Wild-type C57BL/6 mice fed with a matched low fat diet (10% of calories from fat) for 20 weeks (LFD; n=8) or normal chow (WT; n=10) were used as controls for the HFD and Cpt1b groups, respectively.

**MRI/MRS hardware.** All MRI and MRS measurements were performed on a 9.4T horizontal bore MR scanner (Bruker Biospin). For MRI and <sup>1</sup>H MRS, a 35-mm quadrature birdcage coil (Bruker Biospin) was used for both RF transmission and signal reception. For <sup>31</sup>P MRS, a 54-mm linear birdcage coil (Rapid Biomedical) and an actively decoupled surface coil with a diameter of 15 mm were used for transmission and reception, respectively.

**Prospectively-triggered cine MRI.** To assess cardiac systolic function, a prospectively cardiac-triggered FLASH sequence was used to acquire cine images for 5-6 contiguous short axis and 2 long axis slices (thickness: 1 mm). The parameters were: TR/TE: 7/1.8 ms,  $\alpha$ : 15°, matrix: 192x192, FOV: 30x30 mm<sup>2</sup>, frames/cardiac cycle: 15-18, NSA: 6. Left ventricular (LV) lumen was semi-automatically segmented using CAAS MRV 2.0 (Pie Medical) to obtain functional parameters.

**Retrospectively-triggered cine MRI.** To assess cardiac diastolic function, a retrospectively cardiac-triggered FLASH sequence (Intragate) was used to acquire cine images for the midventricular slice, allowing a high temporal resolution of 60 frames per cardiac cycle, as described previously<sup>(2)</sup>. The parameters were: TR/TE: 4.7/2.35 ms,  $\alpha$ : 15°, matrix: 128x128, FOV: 30x30 mm<sup>2</sup>. The LV endocardium excluding papillary muscles was segmented semi-automatically using Segment (version 1.8 R1145, <http://segment.heiberg.se>). From the first derivative of the LV volume-time curve, the early peak filling rate (E) was calculated.

**<sup>1</sup>H MRS.** Localized <sup>1</sup>H MR spectra were acquired during diastole in the interventricular septum (1x2x2 mm<sup>3</sup> voxel) using a cardiac triggered and respiratory gated PRESS sequence, with CHESS water suppression, as described previously<sup>(3)</sup>. The parameters were: TR: ~2s, TE: 9.1ms, 0.41 ms 90° Hermite-shaped excitation pulse, 0.9 ms 180° Mao-type refocusing pulses, 256 scans. Spectral processing and fitting were performed using AMARES in jMRUI<sup>(4)</sup>. Myocardial lipid levels were calculated from the lipid-CH<sub>2</sub> signal relative to the unsuppressed water peak.

**<sup>31</sup>P MRS.** Cardiac-triggered and respiratory-gated <sup>31</sup>P MRS was performed using the image selected *in vivo* spectroscopy (ISIS) sequence on a voxel of typically ~6x6x6 mm<sup>3</sup> covering the left ventricle, at the end of diastolic phase. The parameters were: TR: ~2s, 1.2 ms sinc-shaped excitation pulse, 6.25 ms adiabatic hyperbolic secant inversion pulses, 96 ISIS cycles (768 scans). Localized shimming was performed on the <sup>1</sup>H signal using a 11x11x11 mm<sup>3</sup> PRESS voxel covering the sensitive area of the surface coil. Fitting of the metabolite signals to Lorentzian lineshapes was performed using AMARES in jMRUI<sup>(4)</sup>. The ATP resonances (doublets for  $\gamma$ - and  $\alpha$ -ATP, and a triplet for  $\beta$ -ATP) were fitted with equal amplitudes and line widths within each multiplet, and a J-coupling constant of 17 Hz. The  $\gamma$ -ATP line widths (LW <sub>$\gamma$ -ATP</sub>) were constrained relative to the PCr line widths (LW<sub>PCr</sub>) according to an empirically determined relation: LW <sub>$\gamma$ -ATP</sub> = LW<sub>PCr</sub> + 14.8 Hz (#spectra=63; R=0.78; P<0.001). As a measure of cardiac energy status, the ratio of PCr to  $\gamma$ -ATP was determined and corrected for T<sub>1</sub> partial saturation (correction factor of 1.75 and 1.31 for PCr and  $\gamma$ -ATP, respectively). The ratio was not corrected for the blood ATP signal in the spectra, as data in our lab showed this to be less than 4%.

**Statistical analysis.** All data are presented as means  $\pm$  standard deviation. Statistical differences were analyzed separately between HFD and LFD groups and between Cpt1b and WT groups, respectively, using independent-samples students' T-tests in SPSS 17.0 (SPSS Inc). The level of significance was set at P<0.05 (\*).

**Results:** Myocardial lipid content was higher in HFD compared with LFD, whereas it was not significantly different between Cpt1b and WT (Fig.1). Cardiac energy status was similar between HFD and LFD, while it was significantly lower in Cpt1b compared with WT (Fig. 2). Ejection fraction (EF) was similar among all groups. In contrast, early peak filling rate (E) was lower in both HFD and Cpt1b compared with LFD and WT, respectively (Fig. 3). Normalized LV mass was 12.5% and 7.5% higher in HFD and Cpt1b compared with their respective controls (P<0.05).

**Discussion and Conclusion:** In this study, we investigated myocardial lipid content, energetics, and function in two mouse models of increased fatty acid oxidation. In both mouse models, systolic function (i.e. EF) was preserved, whereas diastolic function (i.e. E) was significantly impaired. Hypertrophy also occurred in both mouse models. In HFD mice, this was associated with increased myocardial lipid accumulation, without a change in cardiac energy status. In Cpt1b mice, on the other hand, diastolic dysfunction was accompanied by a significantly reduced cardiac energy status, without an accumulation of myocardial lipids. In conclusion, both myocardial lipid accumulation and disturbances in cardiac energetics seem to independently contribute to reduced cardiac performance.

**References:** (1) Boudina S, Abel ED. *Physiol.* 2005;21:250-258. (2) Coolen B. *Magn. Res. Med.* 2012; DOI: 10.1002/mrm.24287. (3) Bakermans A. *Circ. Cardiovasc. Imaging.* 2011;4:558-565. (4) Vanhamme L. *J. Magn. Reson.* 1997; 129: 35-43.

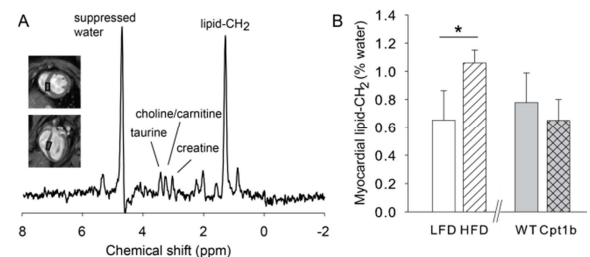


**Figure 1.** (A) Representative cardiac <sup>1</sup>H MR spectrum from the indicated voxel in black, (B) quantification of the lipid-CH<sub>2</sub> signal.

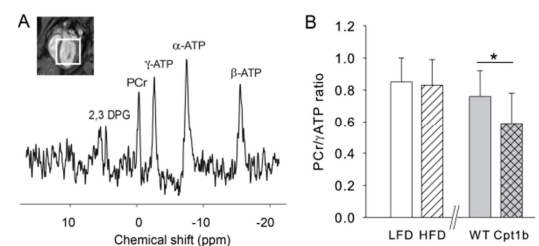


**Figure 2.** (A) Representative cardiac <sup>31</sup>P MR spectrum from the indicated voxel in white, (B) quantification of the PCr/ATP ratio.

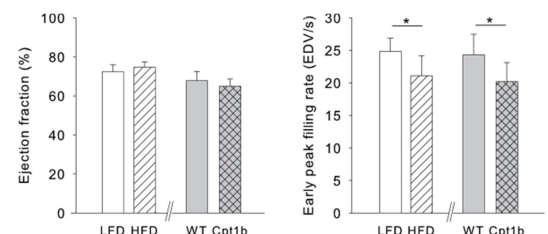


**Figure 3.** Ejection fraction and early peak filling rate.